AAS 16-345

PRECISION ZEM/ZEV FEEDBACK GUIDANCE ALGORITHM UTILIZING VINTI'S ANALYTIC SOLUTION OF PERTURBED KEPLER PROBLEM

Jaemyung Ahn,[*] Yanning Guo,[†] and Bong Wie[‡]

A new implementation of a zero-effort-miss/zero-effort-velocity (ZEM/ZEV) feedback guidance scheme, which utilizes the computational efficiency and accuracy of analytical orbit propagators, is proposed. Kepler's propagator and Vinti's algorithm for the solution of perturbed Kepler problem are used to predict the ZEM and ZEV state vectors and determine the acceleration command, which are often obtained by numerical integration of the equations of motion in the conventional approach. A procedure for optimal time-to-go estimation that can be used with the new guidance algorithm for intercept of moving target is introduced. The effectiveness of the proposed implementation is demonstrated by the performance comparison with the open-loop optimization approach through several case studies.

INTRODUCTION

Guidance of missiles and space vehicles is one of most critical technologies required for their successful mission operations. Various study results on this subject as applied to orbital intercept, rendezvous, and planetary landing problems can be found in the literature. The mathematical methodologies employed by such studies are diverse as well – including the optimal control approaches [1-6], the classical proportional navigation (PN) guidance and its variants [7], and other approaches.

Among these methodologies, the zero-effort-miss/zero-effort-velocity (ZEM/ZEV) feedback guidance and its variants is a practical guidance algorithm that has been extensively examined in the past [8-12]. The generalized ZEM/ZEV guidance scheme [8,9] is physically easy to understand and simple to implement due to its conceptual simplicity. It is a feedback guidance law that can deal with perturbations and/or uncertainties in a robust way – in particular compared with open-loop, optimization-based guidance algorithms.

The performance of the ZEM/ZEV algorithm is satisfactory for various practical applications as well. With an assumption of a uniform gravity field, the algorithm provides a true optimal so-

[*] Associate Professor, Dept. of Aerospace Engineering, KAIST, South Korea. Email: jaemyung.ahn@kaist.ac.kr
[†] Assistant Professor, Dept. of Control Science and Engineering, Harbin Institute of Technology, China. Email: guoyn@hit.edu.cn
[‡] Vance Coffman Endowed Chair Professor, Asteroid Deflection Research Center, Department of Aerospace Engineering, Iowa State University, 2271 Howe Hall, Ames, IA 50011-2271, USA. Email: bongwie@iastate.edu

lution. For some ballistic missile intercept and asteroid intercept scenarios with spherical gravity, it was demonstrated that the ZEM/ZEV approach can even compete with corresponding open-loop optimal solutions, while its feedback characteristics make it more suitable for realistic situations with uncertainties [8-12].

For long-range missions that require the consideration of position-dependent gravity model, however, there are some challenges in using the proposed ZEM/ZEV algorithm. The first challenge is the fast and accurate prediction of the ZEM/ZEV information. Under the assumption of spherical gravitational field (with or without additional perturbations), when the states (position and velocity) of an object at an initial time is specified, it is not possible to express its states at a given time as a closed form in general. For example, for a missile intercept problem presented by Guo et al. [8], the ZEM was computed using a numerical integration of both the interceptor and target missiles. An actual on-board implementation of this numerical integration-based algorithm can be difficult due to the high computational burden.

The second challenge is the determination of terminal time t_f or time-to-go t_{go} for free terminal time problems. Guo et al. [9] proposed a formulation to determine the time-to-go for a Mars landing problem using ZEM/ZEV guidance with an assumption that the direction of gravity vector is constant. Newman [11] developed a series of polynomial equations to determine the terminal time associated with various assumptions on gravity (zero, constant, linear, quadratic, and linearized inverse square) in the context of missile intercept using ZEM (without considering ZEV) guidance. But the authors could not find any previous studies on terminal time (or time-to-go) determination problems for ZEM/ZEV guidance with spherical (or more complex) gravity model.

This paper addresses the aforementioned two challenges by 1) introducing analytic propagators for ZEM/ZEV prediction and 2) developing a formulation to determine the terminal time associated with minimum control-energy guidance problem. The position-dependent gravity model and two analytic propagators – the Kepler propagator (for spherical gravity model) and the Vinti propagator (with additional perturbed gravity model including J_2, J_3, and J_4 terms) [13] – are used. A general formulation to determine the terminal time subject to final position/velocity constraint for a moving target is proposed. Various cases (minimum energy missile intercept, head-on missile intercept, and elliptical orbital rendezvous) will be examined in this paper. The solutions obtained by using the ZEM/ZEV guidance algorithm with terminal time determined using the proposed formula will be compared with the open-loop optimization results to demonstrate its practical effectiveness.

OPTIMAL MISSILE/SPACECRAFT GUIDANCE PROBLEM

Consider the dynamics of a missile or spacecraft, moving in Earth-Centered-Inertial (ECI) coordinate frame, described by

$$\dot{\mathbf{r}} = \mathbf{v} \tag{1}$$

$$\dot{\mathbf{v}} = \mathbf{g}(\mathbf{r}) + \mathbf{a} \tag{2}$$

where **r** and **v** are the position and velocity of the missile, **a** is the acceleration of the missile applied by its propulsion system, and **g** is the gravitational acceleration. Vector **g** is expressed as the function of the position vector $\mathbf{r} = [x, y, z]^T$ as follows:

$$\mathbf{g}(\mathbf{r}) = \mathbf{g}_c(\mathbf{r}) + \mathbf{g}_p(\mathbf{r}) \tag{3}$$

In Eq. (3), $\mathbf{g}_c$ and $\mathbf{g}_p$ respectively denote the spherical (Keplerian) and perturbed gravitational acceleration terms [14-15] described by

$$\mathbf{g}_c(\mathbf{r}) = -\frac{\mu}{r^3}\mathbf{r} \tag{4}$$

$$\mathbf{g}_p(\mathbf{r}) = \begin{pmatrix} \frac{3\mu J_2 R^2}{2r^5}(\frac{5z^2}{r^2}-1)x + \frac{5\mu J_3 R^3 xz}{2r^7}(\frac{7z^2}{r^2}-3) + \frac{15\mu J_4 R^4 x}{8r^7}(1-\frac{14z^2}{r^2}+\frac{21z^4}{r^4}) \\ \frac{3\mu J_2 R^2}{2r^5}(\frac{5z^2}{r^2}-1)y + \frac{5\mu J_3 R^3 yz}{2r^7}(\frac{7z^2}{r^2}-3) + \frac{15\mu J_4 R^4 y}{8r^7}(1-\frac{14z^2}{r^2}+\frac{21z^4}{r^4}) \\ \frac{3\mu J_2 R^2}{2r^5}(\frac{5z^2}{r^2}-3)z + \frac{5\mu J_3 R^3}{2r^5}(\frac{3}{5}-\frac{6z^2}{r^2}+\frac{7z^4}{r^4}) + \frac{15\mu J_4 R^4 z}{8r^7}(5-\frac{70z^2}{3r^2}+\frac{21z^4}{r^4}) \end{pmatrix} \tag{5}$$

In Eqs. (4) and (5), μ is the Earth's gravitational parameter, (J_2, J_3, J_4) are the zonal harmonics terms, and *R* is the equatorial radius of the Earth. Also *r* is the magnitude of position vector **r**.

A missile intercept problem can be defined as a dynamic optimization problem for determining the acceleration history of the missile, **a**, subject to the differential equations describing the interceptor missile's dynamics with a specified objective function and initial/terminal conditions. The objective function *J* is expressed as

$$J = \phi(\mathbf{r}_f, \mathbf{v}_f, t_f) + \int_0^{t_f} f(\mathbf{r}, \mathbf{v}, \mathbf{a}, t)\,dt = \int_0^{t_f} \frac{1}{2}\mathbf{a}^T\mathbf{a}\,dt \tag{6}$$

where $\phi(\mathbf{r}_f, \mathbf{v}_f, t_f)$ is the terminal cost function (set up as zero in this problem).

Initial and terminal conditions of the missile are assumed as

$$\mathbf{r}(0) = \mathbf{r}_{M,0} \tag{7}$$

$$\mathbf{v}(0) = \mathbf{v}_{M,0} \tag{8}$$

$$\mathbf{r}(t_f) = \Theta(t_f) \tag{9}$$

$$\mathbf{v}(t_f) = \Omega(t_f)\ or\ free \tag{10}$$

Note that, for the intercept or rendezvous of a moving target, the final position of the target can be calculated from the target dynamics. It is assumed that the target is moving subject to the gravity only (i.e. free-fall) whose equations of motion are described as

$$\dot{\mathbf{r}}_T = \mathbf{v}_T \tag{11}$$

$$\dot{\mathbf{v}}_T = \mathbf{g}(\mathbf{r}_T) \tag{12}$$

$$\mathbf{r}_T(0) = \mathbf{r}_{T,0},\ \mathbf{v}_T(0) = \mathbf{v}_{T,0} \tag{13}$$

where $\mathbf{r}_T$ and $\mathbf{v}_T$ are the position and velocity of the target, respectively. For an intercept problem, $\Theta(t)$ equals $\mathbf{r}_T(t)$ and the terminal missile velocity is unspecified. For a rendezvous problem, on the other hand, we have to specify both of terminal position and velocities as: $\Theta(t) = \mathbf{r}_T(t)$ and $\Omega(t) = \mathbf{v}_T(t)$.

Now the optimal control problem is completely defined by Eq. (6) (objective function), Eqs. (1)-(2) (dynamic constraints), and Eqs. (7)-(10) (initial and terminal constraints) [16]. To simplify the problem formulation, we may assume that the gravity vector $\mathbf{g}$ is a function of time only ($\mathbf{g}(\mathbf{r}) = \mathbf{g}(t), \mathbf{g}(\mathbf{r}_T) = \mathbf{g}_T(t)$). The Hamiltonian for this problem is then defined as

$$H = \frac{1}{2}\mathbf{a}^T\mathbf{a} + \mathbf{p}_r^T\mathbf{v} + \mathbf{p}_v^T(\mathbf{g}(\mathbf{r}) + \mathbf{a}) \approx \frac{1}{2}\mathbf{a}^T\mathbf{a} + \mathbf{p}_r^T\mathbf{v} + \mathbf{p}_v^T(\mathbf{g}(t) + \mathbf{a}) \tag{14}$$

where $\mathbf{p}_r$ and $\mathbf{p}_v$ are co-state vectors associated with Eqs. (1) and (2), respectively.

The differential equations for the co-states are

$$\dot{\mathbf{p}}_r = -\frac{\partial H}{\partial \mathbf{r}} = \mathbf{0} \tag{15}$$

$$\dot{\mathbf{p}}_v = -\frac{\partial H}{\partial \mathbf{v}} = -\mathbf{p}_r \tag{16}$$

From Eq. (15), we can conclude that $\mathbf{p}_r$ is a constant vector. Using this properties, $\mathbf{p}_v$ is determined as

$$\mathbf{p}_v(t) = -\mathbf{p}_r(t - t_f) + \mathbf{p}_{v,f} \tag{17}$$

where $\mathbf{p}_{v,f} = \mathbf{p}_v(t_f)$ is value of the co-state vector $\mathbf{p}_v$ at terminal time.

The optimality condition for this problem is given as

$$\mathbf{0} = \frac{\partial H}{\partial \mathbf{a}} = \mathbf{a} + \mathbf{p}_v \tag{18}$$

By combining Eqs. (17) and (18), we obtain the optimal acceleration vector as

$$\mathbf{a} = -\mathbf{p}_v = \mathbf{p}_r(t - t_f) - \mathbf{p}_{v,f} = -\mathbf{p}_r \cdot t_{go} - \mathbf{p}_{v,f} \tag{19}$$

where $t_{go} \equiv t_f - t$ is the time-to-go for the intercept.

Equation (19) indicates that the optimal control law for this intercept/rendezvous problem is determined by finding two vectors: $\mathbf{p}_r$ and $\mathbf{p}_{v,f}$. It should be noted that the solution is true optimal under the assumption: $\mathbf{g}(\mathbf{r}) = \mathbf{g}(t), \mathbf{g}(\mathbf{r}_T) = \mathbf{g}_T(t)$.

OPTIMAL FEEDBACK GUIDANCE USING ZEM/ZEV

This section presents a procedure to implement Eq. (19) as a feedback form – the function of current position and velocity. Assume that that the position and velocity of the missile at current time t_0 are respectively $\mathbf{r}(t_0)$ and $\mathbf{v}(t_0)$. From Eq. (2), the velocity of the missile at time *t* is expressed as

$$\mathbf{v}(t) = \mathbf{v}(t_0) + \int_{t_0}^{t} (\mathbf{g}(\tau) + \mathbf{a}(\tau))\, d\tau = \mathbf{v}^{FF}(t) + \int_{t_0}^{t} \mathbf{a}(\tau)\, d\tau \tag{20}$$

where $\mathbf{v}^{FF}(t) \equiv \mathbf{v}(t_0) + \int_{t_0}^{t} \mathbf{g}(\tau) d\tau$ is the free-fall velocity of the missile at *t*. By applying Eq. (19) to Eq. (20), we obtain

$$\mathbf{v}(t) = \mathbf{v}^{FF}(t) - (\mathbf{p}_{v,f} + \mathbf{p}_r \cdot t_f)(t - t_0) + \mathbf{p}_r \cdot (t^2 - t_0^2)/2 \tag{21}$$

The terminal velocity of the missile is expressed as

$$\mathbf{v}_f = \mathbf{v}^{FF}(t_f) - \mathbf{p}_{v,f} \cdot t_{go} - \frac{1}{2}\mathbf{p}_r t_{go}^2 \tag{22}$$

The terminal position of the missile $\mathbf{r}(t_f)$ can be obtained by substituting Eq. (21) into Eq. (1) as

$$\mathbf{r}_f = \mathbf{r}(t_0) + \int_{t_0}^{t_f} \mathbf{v}(\tau)\,d\tau = \mathbf{r}(t_0) + \int_{t_0}^{t_f} \left(\mathbf{v}^{FF}(\tau) - (\mathbf{p}_{v,f} + \mathbf{p}_r t_f)(\tau - t_0) + \mathbf{p}_r(\tau^2 - t_0^2)/2\right) d\tau \tag{23}$$

By evaluating the integral in Eq. (23), we obtain the following result:

$$\mathbf{r}_f = \mathbf{r}(t_0) + \int_{t_0}^{t_f} \mathbf{v}^{FF}(\tau)\,d\tau - \frac{1}{2}t_{go}^2\mathbf{p}_{v,f} - \frac{1}{3}t_{go}^3\mathbf{p}_r = \mathbf{r}^{FF}(t_f) - \frac{1}{2}t_{go}^2\mathbf{p}_{v,f} - \frac{1}{3}t_{go}^3\mathbf{p}_r \tag{24}$$

where $\mathbf{r}^{FF}(\tau) \equiv \mathbf{r}(t_0) + \int_{t_0}^{\tau} \mathbf{v}^{FF}(s)\,d\tau$ is the free-fall position of the missile. Note that the expressions for $\mathbf{v}^{FF}$ and $\mathbf{r}^{FF}$ not exact because the gravitational acceleration is the function of its position that is affected by the control acceleration **a**. In this paper, we assumed that **g** is the function of time and used these expressions.

Let us define the zero-effort-miss (ZEM) and the zero-effort-velocity (ZEV) as

$$\mathbf{ZEM} \equiv \Theta(t_f) - \mathbf{r}^{FF}(t_f) \tag{25}$$

$$\mathbf{ZEV} \equiv \Omega(t_f) - \mathbf{v}^{FF}(t_f) \tag{26}$$

Equations (22) and (24) are combined with the terminal conditions, Eqs. (9) and (10), to determine the two vectors $\mathbf{p}_r$ and $\mathbf{p}_{v,f}$. Two types of problem with different terminal conditions are considered. In this section, we assume that the final time t_f is given.

Type 1: Terminal position and velocity on a curve ($\mathbf{r}_f = \Theta(t_f), \mathbf{v}_f = \Omega(t_f)$)

From Eqs. (22) and (24), we have the two set of linear equations for $\mathbf{p}_r$ and $\mathbf{p}_{v,f}$, as follows:

$$\mathbf{r}_f - \mathbf{r}^{FF}(t_f) = \Theta(t_f) - \mathbf{r}^{FF}(t_f) = \mathbf{ZEM} = \left(-\frac{1}{2}t_{go}^2\right)\cdot\mathbf{p}_{v,f} + \left(-\frac{1}{3}t_{go}^3\right)\cdot\mathbf{p}_r \tag{27}$$

$$\mathbf{v}_f - \mathbf{v}^{FF}(t_f) = \Omega(t_f) - \mathbf{v}^{FF}(t_f) = \mathbf{ZEV} = \left(-t_{go}\right)\cdot\mathbf{p}_{v,f} + \left(-\frac{1}{2}t_{go}^2\right)\cdot\mathbf{p}_r \tag{28}$$

By solving these equations, we can determine $\mathbf{p}_r$ and $\mathbf{p}_{v,f}$ as

$$\mathbf{p}_{v,f} = -\frac{4}{t_{go}}\mathbf{ZEV} + \frac{6}{t_{go}^2}\mathbf{ZEM} \tag{29}$$

$$\mathbf{p}_r = \frac{6}{t_{go}^2}\mathbf{ZEV} - \frac{12}{t_{go}^3}\mathbf{ZEM} \tag{30}$$

When Eqs. (29) and (30) are applied to Eq. (19), we have the optimal control law for **Type 1** of the form:

$$\mathbf{a}^* = -\frac{2}{t_{go}}\mathbf{ZEV} + \frac{6}{t_{go}^2}\mathbf{ZEM} \tag{31}$$

Type 2: Terminal position specified on a curve, terminal velocity free ($\mathbf{r}_f = \Theta(t_f)$)

If the terminal velocity is free, the terminal co-state associated with velocity can be determined as

$$\mathbf{p}_v(t_f) = \mathbf{p}_{v,f} = \frac{\partial \phi}{\partial \mathbf{v}_f} = \mathbf{0} \tag{32}$$

From Eq. (24), $\mathbf{p}_r$ is determined as

$$\mathbf{p}_r = -\frac{3}{t_{go}^3}\mathbf{ZEM} \tag{33}$$

Finally, we can obtain the optimal control law for **Type 2** as

$$\mathbf{a}^* = \frac{3}{t_{go}^2}\mathbf{ZEM} \tag{34}$$

Calculation of ZEM and ZEV

It should be noted that the optimal control laws for both cases use the ZEM/ZEV information, which require the free-fall position and velocity vectors ($\mathbf{r}^{FF}(t_f)$, $\mathbf{v}^{FF}(t_f)$). Different methodologies can be used to obtain these ZEM/ZEV values. As the simplest (and computationally least expensive) approach, we can derive the analytic expressions for $\mathbf{r}^{FF}(t_f)$ and $\mathbf{v}^{FF}(t_f)$ under the assumption of uniform gravity: $\mathbf{g}(\mathbf{r}) = \mathbf{g}$ = a constant vector. In this case, the ZEM and ZEV are expressed as follows:

$$\begin{aligned}\mathbf{ZEM} &= \Theta(t_f) - (\mathbf{r} + t_{go}\cdot\mathbf{v} + \frac{1}{2}t_{go}^2\cdot\mathbf{g}) \\ &= (\mathbf{r}_T - \mathbf{r}) + t_{go}\cdot(\mathbf{v}_T - \mathbf{v}) \quad \text{(free-fall target)}\end{aligned} \tag{35}$$

$$\begin{aligned}\mathbf{ZEV} &= \Omega(t_f) - (\mathbf{v} + t_{go}\cdot\mathbf{g}) \\ &= \begin{cases} \mathbf{v}_T - \mathbf{v} & \text{(rendezvous)} \\ -(\mathbf{v}_T + \mathbf{v}) - 2t_{go}\cdot\mathbf{g} & \text{(special head-on intercept)} \end{cases}\end{aligned} \tag{36}$$

While this approach with constant gravity assumption works fine for relatively short-range missions, its effectiveness is reduced for missions with longer ranges in which the changes in the direction of gravity is not negligible. A straightforward modification of Eqs. (35)-(36) would be the method of direct integration used in [8]. In this approach, the free-fall position and velocity are obtained by numerically integrating Eqs. (1)-(2) until the final time t_f with $\mathbf{a} = \mathbf{0}$. Similarly, the target's position and velocity are obtained by numerical integration of Eqs. (11)-(12). The advantage of this approach is its flexibility – the effects of non-spherical gravity terms (and even atmospheric drag) can be included. However, the high computational resource consumption required for the numerical integration can make it prohibitively difficult to be implemented on-board.

Analytic propagators can be considered as the third alternative, which is used in this paper. We consider two different propagators: Kepler's propagator and Vinti's propagator. The Kepler's propagator computes the ZEM and ZEV by solving Kepler's initial value problem (with spherical gravity assumption) for both of the missile and target. The solution of the Kepler's problem is expressed as

$$\begin{pmatrix} \mathbf{r}^{FF}(t_f) \\ \mathbf{v}^{FF}(t_f) \end{pmatrix} = \begin{bmatrix} f & g \\ \dot{f} & \dot{g} \end{bmatrix} \begin{pmatrix} \mathbf{r} \\ \mathbf{v} \end{pmatrix} \tag{37}$$

where f, g, $\dot{f}$, and $\dot{g}$ can be obtained by various methods such as iteration and series solution [14-15]. The Vinti's propagator applies the *Vinti Spheroidal Method* to refine the solution of Kepler's initial value problem so that the effects of zonal harmonics (J_2, J_3, and J_4 terms) are included [13].

DETERMINATION OF TERMINAL TIME

The ZEM/ZEV guidance laws expressed in Eqs. (31) and (34) are derived with an assumption that the terminal time t_f is specified. This section introduces a formula to determine t_f for terminal time free problems. Note that the problems discussed in the previous section have terminal boundary conditions that a subset of terminal state $\mathbf{x}_s$ are specified on a curve $\Psi(t)$. Following [16], the terminal boundary conditions for the optimal control problem with this situation are described as

$$\mathbf{x}_s(t_f) = \Psi(t_f) \tag{38}$$

$$H\Big|_{t_f} + \frac{\partial \phi(\mathbf{x}_f, t_f)}{\partial t_f} + \left(\frac{\partial \phi(\mathbf{x}_f, t_f)}{\partial \mathbf{x}_s} - \mathbf{p}_s(t_f) \right)^T \left(\frac{d\Psi(t)}{dt} \right)_{t_f} = 0 \tag{39}$$

$$\mathbf{p}_{s^c}(t_f) = \mathbf{0} \tag{40}$$

where $\phi(\mathbf{x}_f, t_f)$ is the terminal cost function, $\mathbf{p}_s$ is the co-state vector associated with $\mathbf{x}_s$, and $\mathbf{p}_{s^c}$ is the co-state vector associated with unspecified states at t_f. These equations are customized for Type 1 and Type 2 to derive the relationships that should be satisfied at terminal time, which is used to determine t_f.

Type 1: Terminal position and velocity on a curve ($\mathbf{r}_f = \Theta(t_f), \mathbf{v}_f = \Omega(t_f)$)

In this case, vector $\mathbf{x}_s$ is composed of the whole states as $\mathbf{x}_s = [\mathbf{r}^T \ \mathbf{v}^T]^T$. The terminal cost function is zero ($\phi = 0$) for this problem, and Eq. (39) becomes

$$\left[H - \mathbf{p}_r^T \left(\frac{d\Theta}{dt} \right) - \mathbf{p}_v^T \left(\frac{d\Omega}{dt} \right) \right]_{t_f} = 0 \tag{41}$$

By applying Eq. (14) to Eq. (41), we obtain the following relationship:

$$\left[H\right]_{t_f} = \frac{1}{2}\mathbf{a}(t_f)^T\mathbf{a}(t_f) + \mathbf{p}_r^T\mathbf{v}_f + \mathbf{p}_{v,f}^T(\mathbf{a}(t_f) + \mathbf{g}(t_f)) = \mathbf{p}_r^T \cdot \dot{\Theta}(t_f) + \mathbf{p}_{v,f}^T \cdot \dot{\Omega}(t_f) \tag{42}$$

From Eq. (17), the terminal acceleration and is expressed as

$$\mathbf{a}(t_f) = -\mathbf{p}_{v,f} \tag{43}$$

We obtain the terminal velocity $\mathbf{v}_f$ from Eq. (22). Also note that the time-to-go t_{go} becomes the terminal time t_f if it is evaluated at $t = 0$. Then, Eq. (42) is reformulated as

$$f(t_f) = \frac{1}{2}(\mathbf{p}_{v,f} + t_f\mathbf{p}_r)^T(\mathbf{p}_{v,f} + t_f\mathbf{p}_r) + \mathbf{p}_r^T[\dot{\Theta}(t_f) - \mathbf{v}^{FF}(t_f)] + \mathbf{p}_{v,f}^T[\dot{\Omega}(t_f) - \mathbf{g}(t_f)] = 0 \tag{44}$$

where $\mathbf{p}_r$ and $\mathbf{p}_{v,f}$ are expressed using ZEM, ZEV, and t_f by replacing t_{go} in Eqs. (29)-(30) by t_f.

The optimal terminal time can be obtained by solving Eq. (44) for t_f. The Newton-Raphson method can be used to iterate on t_f as

$$t_f^{(n+1)} = t_f^n + \Delta t_f = t_f^n - \frac{f(t_f^n)}{f'(t_f^n)} \tag{45}$$

where t_f^k denotes the predicted value of t_f at k^{th} iteration. The derivative f' is expressed as

$$\begin{aligned} f'(t_f) = &\left(\frac{d\mathbf{p}_{v,f}}{dt_f} + \mathbf{p}_r + \frac{d\mathbf{p}_r}{dt_f}t_f\right)^T\left(\mathbf{p}_{v,f} + t_f\mathbf{p}_r\right) \\ &+ \left(\frac{d\mathbf{p}_r}{dt_f}\right)^T\left(\dot{\Theta}(t_f) - \mathbf{v}^{FF}(t_f)\right) + \mathbf{p}_r^T\left(\ddot{\Theta}(t_f) - \mathbf{g}(\mathbf{r}_f)\right) \\ &+ \left(\frac{d\mathbf{p}_{v,f}}{dt_f}\right)^T\left(\dot{\Omega}(t_f) - \mathbf{g}(\mathbf{r}^{FF}(t_f)\right) + \mathbf{p}_{v,f}^T\left(\ddot{\Omega}(t_f) - \frac{d}{dt_f}\mathbf{g}(\mathbf{r}_f)\right) \end{aligned} \tag{46}$$

where the derivatives are described by

$$\frac{d\mathbf{p}_{v,f}}{dt_f} = \frac{4}{t_f^2}\mathbf{ZEV} - \frac{4}{t_f}\frac{d(\mathbf{ZEV})}{dt_f} - \frac{12}{t_f^3}\mathbf{ZEM} + \frac{6}{t_f^2}\frac{d(\mathbf{ZEM})}{dt_f} \tag{47}$$

$$\frac{d\mathbf{p}_r}{dt_f} = -\frac{12}{t_f^3}\mathbf{ZEV} + \frac{6}{t_f^2}\frac{d(\mathbf{ZEV})}{dt_f} + \frac{36}{t_f^4}\mathbf{ZEM} - \frac{12}{t_f^3}\frac{d(\mathbf{ZEM})}{dt_f} \tag{48}$$

$$\begin{aligned} \frac{d}{dt_f}\mathbf{g}(t_f) &= \frac{\mu}{\left\|\mathbf{r}(t_f)\right\|^5}\left(3\left(\mathbf{r}(t_f)\cdot\mathbf{v}(t_f)\right)\mathbf{r}(t_f) - \left(\mathbf{r}(t_f)\cdot\mathbf{r}(t_f)\right)\mathbf{v}(t_f)\right) \\ &= \frac{\mu}{\left\|\Theta(t_f)\right\|^5}\left(3\left(\Theta(t_f)\cdot\Omega(t_f)\right)\Theta(t_f) - \left(\Theta(t_f)\cdot\Theta(t_f)\right)\Omega(t_f)\right) \end{aligned} \tag{49}$$

$$\frac{d(\mathbf{ZEM})}{dt_f} = \dot{\Theta}(t_f) - \mathbf{v}^{FF}(t_f) \tag{50}$$

$$\frac{d(\mathbf{ZEV})}{dt_f} = \dot{\Omega}(t_f) - \mathbf{g}(\mathbf{r}^{FF}(t_f)) \tag{51}$$

Note that the terminal position and velocity constraints, $\mathbf{r}_f = \Theta(t_f)$ and $\mathbf{v}_f = \Omega(t_f)$, are used to evaluate $\mathbf{g}(t_f)$ and $d(\mathbf{g}(t_f))/dt_f$ in Eqs. (44) and (46).

Type 2: Terminal position specified on a curve, terminal velocity free ($\mathbf{r}_f = \Theta(t_f)$)

When the terminal velocity is free, vector $\mathbf{x}_s$ is defined as $\mathbf{x}_s = \mathbf{r}$. Similar to Eq. (41), we can set up an equation to obtain the terminal time associated with the boundary condition as

$$\left[H - \mathbf{p}_r^T \left(\frac{d\Theta}{dt} \right) \right]_{t_f} = 0 \tag{52}$$

In addition, because the terminal velocity is free, from Eq. (40), the terminal co-state associated with velocity becomes zero as

$$\mathbf{p}_v(t_f) = \mathbf{p}_{v,f} = \mathbf{0} \tag{53}$$

This leads to the zero terminal acceleration ($\mathbf{a}(t_f) = -\mathbf{p}_{v,f} = \mathbf{0}$, from Eq. (17)). Then, Eq. (52) is rearranged as

$$\mathbf{p}_r^T(\dot{\Theta}(t_f) - \mathbf{v}_f) = 0 \tag{54}$$

If we evaluate this equation at $t = 0$, $\mathbf{p}_r$ and $\mathbf{v}_f$ are expressed using ZEM, t_f, and $\mathbf{v}^{FF}(t_f)$ by replacing t_{go} in Eqs. (22) and (33) by t_f. Then Eq. (54) becomes the following root-finding problem for t_f:

$$f(t_f) = \mathbf{ZEM}^T(\dot{\Theta}(t_f) - \mathbf{v}^{FF}(t_f) - \frac{3}{2t_f}\mathbf{ZEM}) = 0 \tag{55}$$

The analytic derivative used for the Newton-Raphson iteration to solve Eq. (55) is expressed as

$$\begin{aligned} f'(t_f) = &\left[\frac{d(\mathbf{ZEM})}{dt_f} \right]^T \left(\dot{\Theta}(t_f) - \mathbf{v}^{FF}(t_f) - \frac{3}{2t_f}\mathbf{ZEM} \right) \\ &+ \mathbf{ZEM}^T \left(\ddot{\Theta}(t_f) - \mathbf{g}\left(\mathbf{r}^{FF}(t_f)\right) + \frac{3}{2t_f^2}\mathbf{ZEM} - \frac{3}{2t_f}\frac{d(\mathbf{ZEM})}{dt_f} \right) \end{aligned} \tag{56}$$

where $d(\mathbf{ZEM})/dt_f$ is defined in Eq. (50).

The Newton-Raphson iteration to solve Eqs. (44) and (55) using the analytic derivative expressed in Eqs. (46)-(51) and (56) converges very fast. This procedure can be effectively used to determine the terminal time at the initial phase of the intercept, or even during midcourse guidance procedure to update the terminal time – as the outer loop of the main ZEM guidance loop.

CASE STUDIES

This section presents four case studies (Cases A, B, C, and D) for missile and spacecraft intercept/rendezvous problems using the proposed ZEM/ZEV guidance law and/or optimal t_f selection procedure. The first two cases are t_f free, minimum energy, missile intercept problems where the final position constraint is imposed. In Case A, the terminal velocity constraint is not applied (ZEM guidance). A special case of direct intercept condition (i.e. the sum of velocity vectors of the interceptor and target is zero) is imposed as the terminal velocity constraint of Case B (ZEM/ZEV guidance). The next two cases are satellite intercept/rendezvous problems. Case C solved a t_f free, minimum energy, satellite intercept problem (ZEM guidance), and finally a series of t_f fixed, minimum energy, satellite rendezvous problems (ZEM/ZEV guidance) with various t_f values are dealt with in Case D.

For each case study, the ZEM/ZEV guidance simulation using the proposed methodology was compared with the open-loop trajectory optimization result. MATLAB was used for the implementation of the ZEM/ZEV guidance simulation, and the open-loop trajectory optimization was conducted using GPOPS-II software that operates based on the Gauss pseudo-spectral method [17]. Analytic orbital propagators were implemented using MATLAB translations of the FORTRAN sources provided by Dr. Gim Der of Der Astrodynamics [18].

Case A: Terminal position specified (Minimum Energy Intercept)

The subject of the first case study is selected as a ballistic missile intercept problem presented in [8]. The dynamics of the intercept missile and the target missile are expressed as Eqs. (1)-(2) and Eqs. (11)-(12), respectively. In this case, only the terminal position constraint is imposed and the constraining curve is defined as the position of the target missile ($\Theta(t) = \mathbf{r}_T(t)$). The initial conditions for the interceptor and target missiles are presented in Table 1.

Table 1: Initial Conditions of Interceptor and Target Missiles (Cases A and B)

	Interceptor	**Target**
Initial Position (km, km, km)	$\mathbf{r}_{0_M}$ = [0.0, 4510.1, 4510.1]^T	$\mathbf{r}_{0_T}$ = [0.0, 0.0, 6378.2]^T
Initial Velocity (km/s, km/s, km/s)	$\mathbf{v}_{0_M}$ = [0.0, 2.006, 5.954]^T	$\mathbf{v}_{0_T}$ = [0.0, 6.785, 2.880]^T

Figure 1 shows the trajectories of the interceptor and target missiles for this case obtained by the ZEM guidance simulation and the open-loop optimization. It can be seen that the two trajectories almost coincide, which suggests that the ZEM guidance produces almost the same result as the open-loop optimization. The final time t_f for the ZEM guidance was determined as 705.8 s (Kepler) / 706.2 s (Vinti) by solving the root finding problem $f(t_f) = 0$ expressed in Eq. (55). The function $f(t_f)$ is presented in the top plot of Figure 2. The final time obtained from the optimization was 700.3 s., which is almost the same as the value for ZEM guidance. The objective function and the acceleration profiles from the two approaches are exhibited in the bottom plots of Figure 2. The curves show almost no difference as well, which indicates the performance of the two approaches for this case are almost identical. The performance summary for the two methods

is presented in Table 1. The performance difference caused by using different analytic propagators was very small.

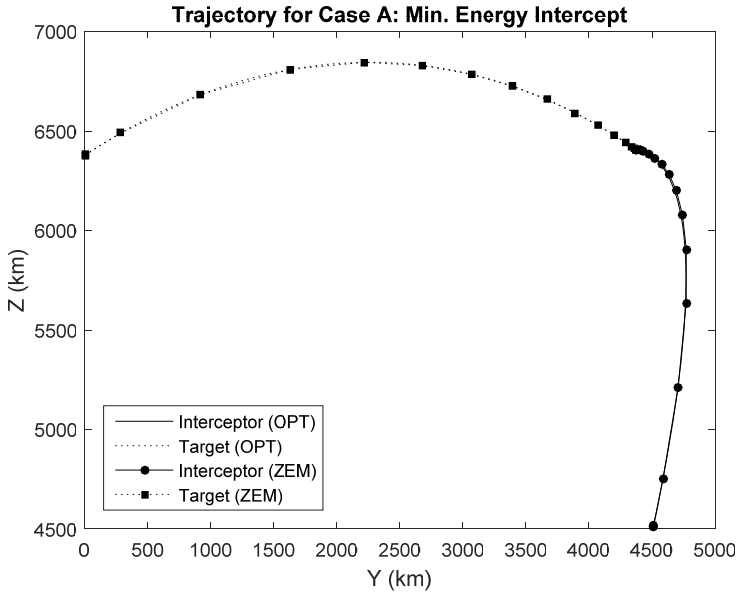

Figure 1: Trajectory for Case A - minimum energy missile intercept

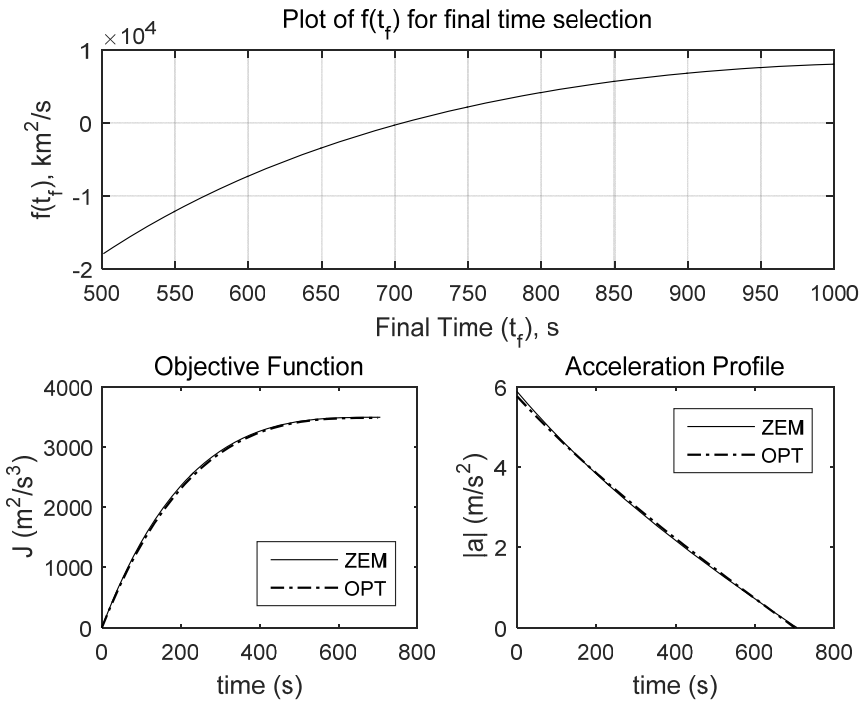

Figure 2: Plots of $f(t_f)$, objective function, and acceleration for Case A

Table 2: Performance summary – Open-loop Optimization vs. ZEM (Case A)

	Open-Loop Optimization	ZEM, predicted t_f (Propagator: Kepler)	ZEM, predicted t_f (Propagator: Vinti)
Terminal time (t_f), *s*	700.3	705.8	706.2
Max. Acceleration, m/s^2	5.76	5.88	5.85
Objective function (J), m^2/s^3	3,483	3,492	3,493

Case B: Terminal velocity and position specified (Head-On Collision Intercept)

This case represents a special case of the head-on intercept in which the velocity of the interceptor is exactly the opposite of target's velocity at the final time. The curve for the terminal position constraint and the terminal velocity constraint are given as $\Theta(t) = \mathbf{r}_T(t)$ and $\Omega(t) = -\mathbf{v}_T(t)$, respectively. The initial conditions for Case A are used in this case as well (presented in Table 1).

The interceptor and target missile trajectories obtained by the ZEM/ZEV guidance simulation and the open-loop optimization are plotted together in Figure 3. The two trajectories are almost the same as each other. The solution of Eq. (44) yields the final time for ZEM/ZEV guidance (Kepler: 581. 7 s / Vinti: 582.3 s), which is very similar to the value obtained from optimization (580.5 s). The top plot of Figure 4 shows the curve used to determine t_f for ZEM/ZEV guidance.

Plots comparing the objective function and acceleration profiles for two approached are presented in the bottom plots of Figure 4 and the summary of performance comparison is provided in Table 3. Both of them indicate that the proposed guidance works almost as effective as the open-loop optimal solution. Like Case A, The performance difference caused by using different analytic propagators was very small.

Table 3: Performance summary – Open-loop Optimization vs. ZEM/ZEV (Case B)

	Open-Loop Optimization	ZEM/ZEV, predicted t_f (Propagator: Kepler)	ZEM/ZEV, predicted t_f (Propagator: Vinti)
Terminal time (t_f), *s*	580.5	581.7	582.3
Max. Acceleration, m/s^2	14.6	15.3	14.6
Objective function (J), m^2/s^3	25,337	25,356	25,369

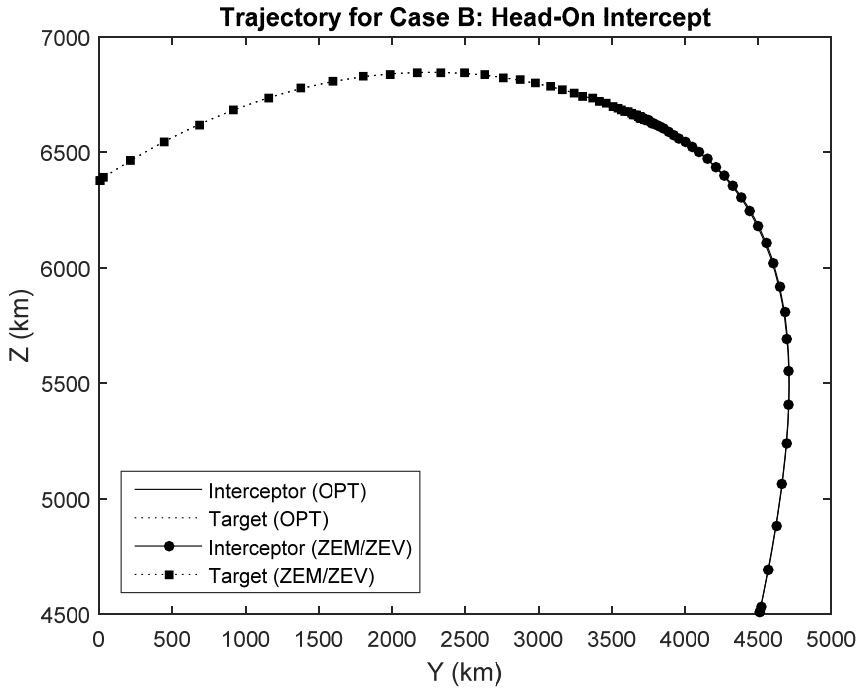

Figure 3: Trajectory for Case B – head-on collision intercept

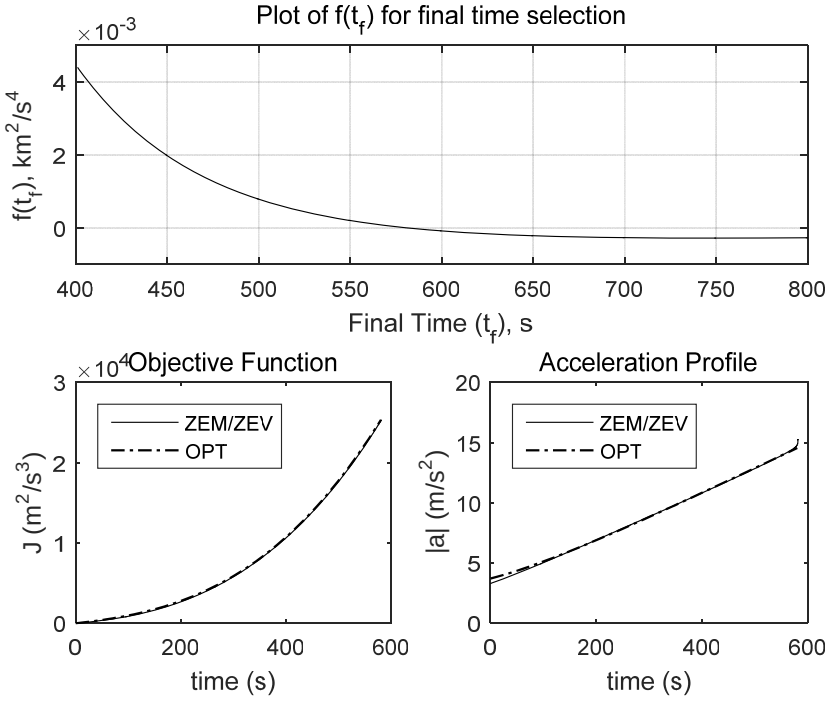

Figure 4: Plots of $f(t_f)$, objective function, and acceleration for Case B

Case C: Terminal position specified (Chasing type intercept, free terminal time)

Case C is similar to Case A in that only the final position is specified, but the difference is that the directions of initial velocity vectors of target and interceptor spacecraft are the same. The target satellite is in an equatorial orbit with perigee/apogee altitudes of 700 km / 1,000 km. The interceptor satellite orbit is a circular orbit with an inclination angle of 15 degrees. The initial conditions and orbital parameters are provided in Table 4.

Table 4: Initial Conditions of Interceptor and Target Satellites (Cases C and D)

	Interceptor Satellite	**Target Satellite**
Initial Position (km, km, km)	$\mathbf{r}_{0_M} = [-6643.8, 0.0, -1780.2]^T$	$\mathbf{r}_{0_T} = [-7078.1, 0.0, 0.0]^T$
Initial Velocity (km/s, km/s, km/s)	$\mathbf{v}_{0_M} = [0.0, -7.613, 0.0]^T$	$\mathbf{v}_{0_T} = [0.0, -7.582, 0.0]^T$
Orbital Parameters		
Perigee Altitude (km)	700	500
Apogee Altitude (km)	1,000	500
Inclination (deg.)	0	15

The trajectories obtained by the two methods are presented in Figure 5. The solution of the root-finding problem expressed in Eq. (55) is solved to obtain the final time t_f = 1,486 seconds. The optimal final time from numerical optimization was 1,469 s (Kepler) / 1,465 s (Vinti) – approximately 1% smaller than the value found by the proposed method. The top plot of Figure 6 shows the function $f(t_f)$ expressed in Eq. (55).

The bottom plots of Figure 6 compare the objective function and acceleration profiles for the two approaches. While the profiles are very similar, unlike Cases A and B, we can observe the differences in two curves for both profiles. The difference (although small) can be attributed to the longer flight time of Case C (~1,500 sec.) compared with the previous two cases (500 – 700 sec.). The performance comparison for two approaches are summarized in Table 5. The performance difference caused by using different analytic propagators was negligible in Case C, too.

Table 5: Performance summary – Open-loop Optimization vs. ZEM/ZEV (Case C)

	Open-loop Optimization	ZEM/ZEV, predicted t_f (Propagator: Kepler)	ZEM/ZEV, predicted t_f (Propagator: Vinti)
Terminal time (t_f), *s*	1,486	1,469	1,465
Max. Acceleration, m/s^2	0.79	0.87	0.87
Objective function (J), m^2/s^3	102.8	105.6	105.9

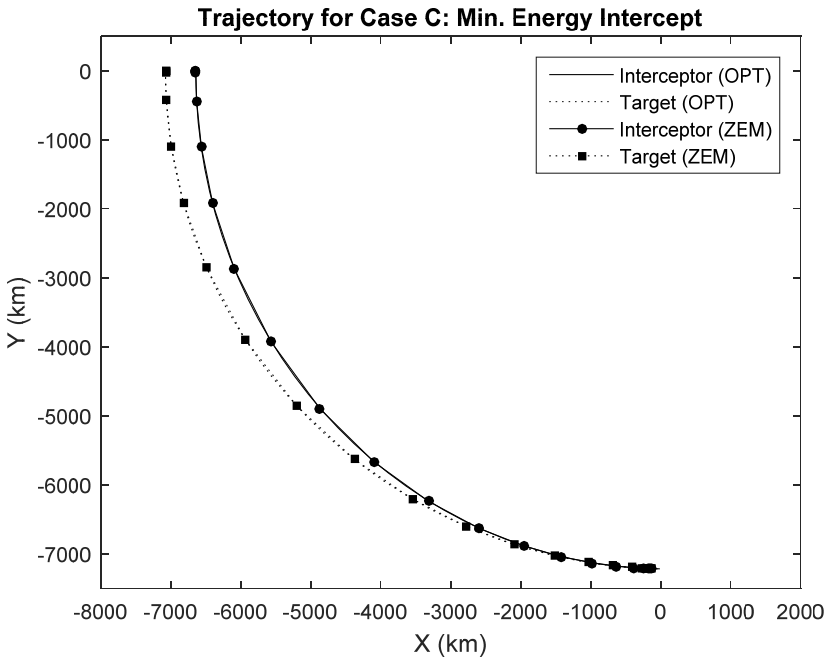

Figure 5: Trajectory for Case C – minimum energy intercept

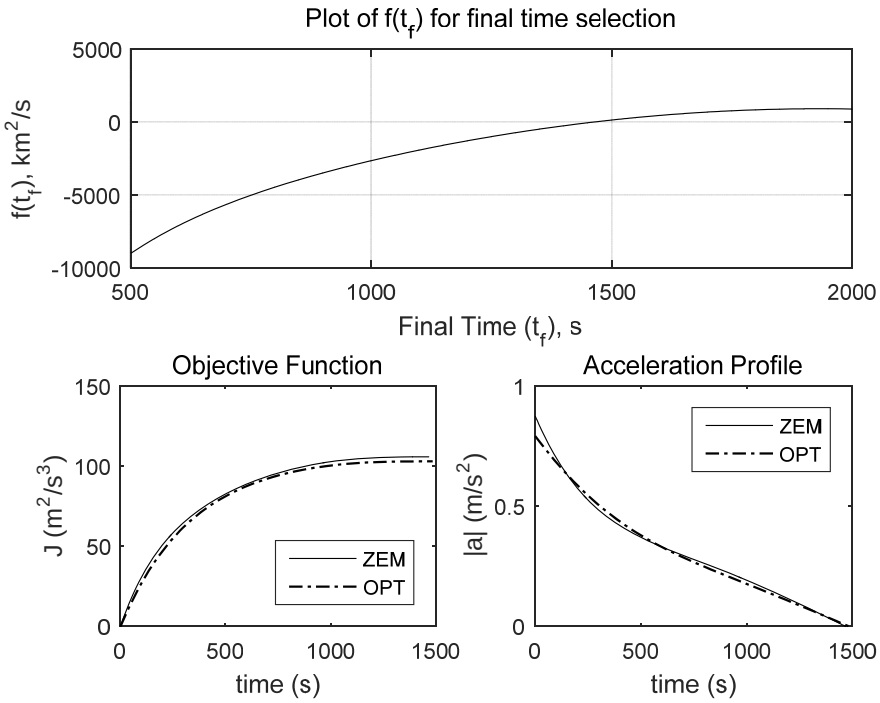

Figure 6: Plots of $f(t_f)$, objective function, and acceleration for Case C

Case D: Terminal velocity and position specified (rendezvous, fixed terminal time)

The last case is concerned with a rendezvous problem between two spacecraft. Initial conditions for the interceptor and target spacecraft are the same as those for Case C. The curves for the final position and velocity are the position and velocity of the target spacecraft, respectively ($\Theta(t) = \mathbf{r}_T(t), \Omega(t) = \mathbf{v}_T(t)$). Figure 7 presents the plots of $f(t_f)$ and $f'(t_f)$. It can be observed that there is no t_f value that satisfies the relationship $f(t_f) = 0$. Two different situations can cause this. First, the optimal trajectory for the rendezvous with minimum control energy would require very long operation time and range. This can result in a very large change in the direction of gravity vector, and the calculation of the optimal t_f using Eq. (44) can fail. Secondly, it is also possible that this rendezvous problem actually does not have a finite optimal t_f value (i.e. the larger t_f, the smaller *J*). Further analysis is required to determine the true cause of failure in root-finding. The issue can be resolved by adding the terminal-time minimization term to the objective function as $J = \int_0^{t_f} (\Gamma + \mathbf{a}^T\mathbf{a} \,/\, 2)\, dt$ [3]. Note that, to apply the ZEM/ZEV guidance with this objective function, the transversality condition described in Eqs. (42) and (55) should be modified as well, which will be conducted as a future study.

Table 6 summarizes the results of ZEM/ZEV guidance simulations and open-loop optimizations for different t_f values (final time specified). Performance indices and maximum accelerations of the ZEM/ZEV guidance simulations for various final time (500 – 5,500 sec.) is compared with those from open-loop optimizations. For missions with relatively short ranges, the ZEM/ZEV feedback guidance performs almost the same as the open-loop optimization. This can be observed in Figure 8 and the top plots of Figure 10, which shows the rendezvous trajectory, the cost function, and the acceleration profile for final time of 1,000 seconds. The difference becomes significant for longer mission times. In addition, while the ZEM/ZEV has its minimum cost around t_f = 5,000 sec., the objective function of the open-loop optimization keep decreasing. While the root cause of this phenomenon should be further investigated, one of possible explanation would be that the inaccuracy in the prediction of ZEM/ZEV due to the effect of **a**(*t*) results in the degradation in the performance. The performance difference caused by using different analytic propagators was negligible for relatively short missions, but for very long mission like the condition for t_f = 5,500 s, the difference got increased.

Table 6: Performance comparison – ZEM/ZEV guidance vs. Open-loop optimization

t_f, *s*	500	1,000	1,500	2,000	2,500	3,000	3,500	4,000	4,500	5,000	5,500
J^{OPT}, m²/ s³	152,420	16.431	4,185	1,847	1,353	1,285	1,246	1,116	921	752	665
J^{ZEM} (Kepler), m²/s³	152,420	16,444	4,225	1,958	1,604	1,752	1,978	2,025	1,660	1,116	2,652
J^{ZEM} (Vinti), m²/s³	152,420	16,445	4,227	1,962	1,611	1,763	1,991	2,034	1,655	1,116	2,862
$a_{\max}^{OPT}$, m/s²	43.5	10.5	4.28	2.00	0.84	0.27	0.56	1.15-	0.95	0.76	0.65
$a_{\max}^{ZEM}$ (Kepler), m/s²	43.7	11.0	5.00	2.91	1.94	1.79	1.89	1.79	1.60	1.41	2.51
$a_{\max}^{ZEM}$ (Vinti), m/s²	43.8	11.0	5.01	2.93	1.96	1.80	1.89	1.79	1.59	1.41	2.59

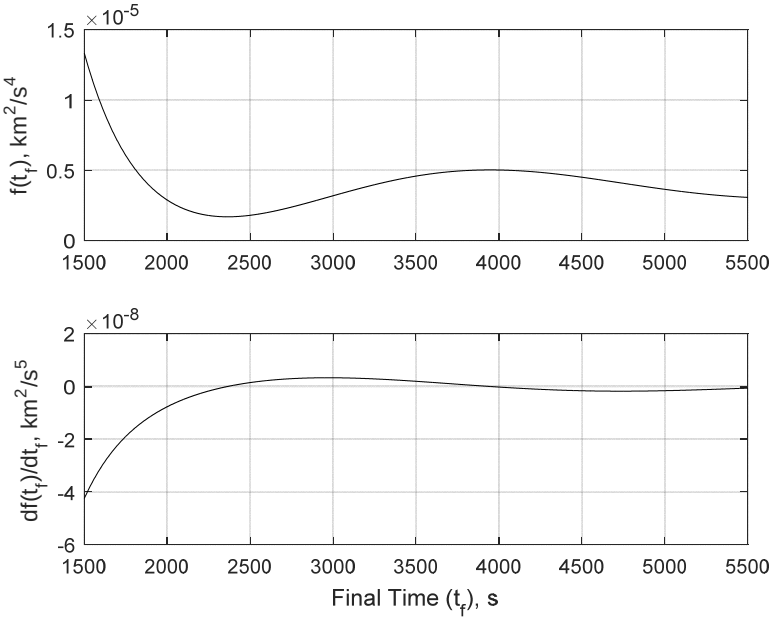

Figure 7: Plots of $f(t_f)$ and $f'(t_f)$ for Case D

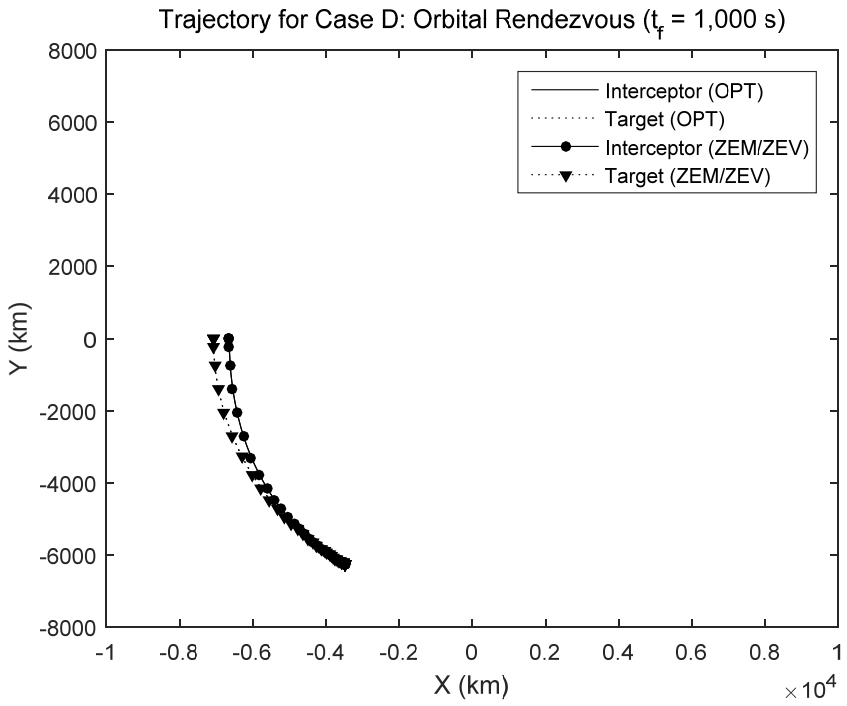

Figure 8: Trajectory for Case D – orbital rendezvous (t_f = 1,000 sec.)

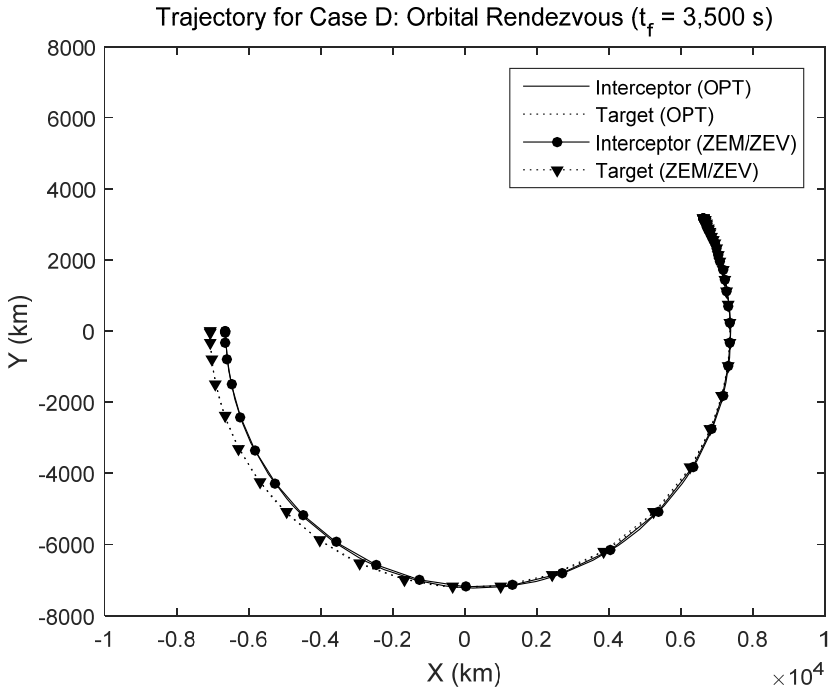

Figure 9: Trajectory for Case D – orbital rendezvous (t_f = 3,500 sec.)

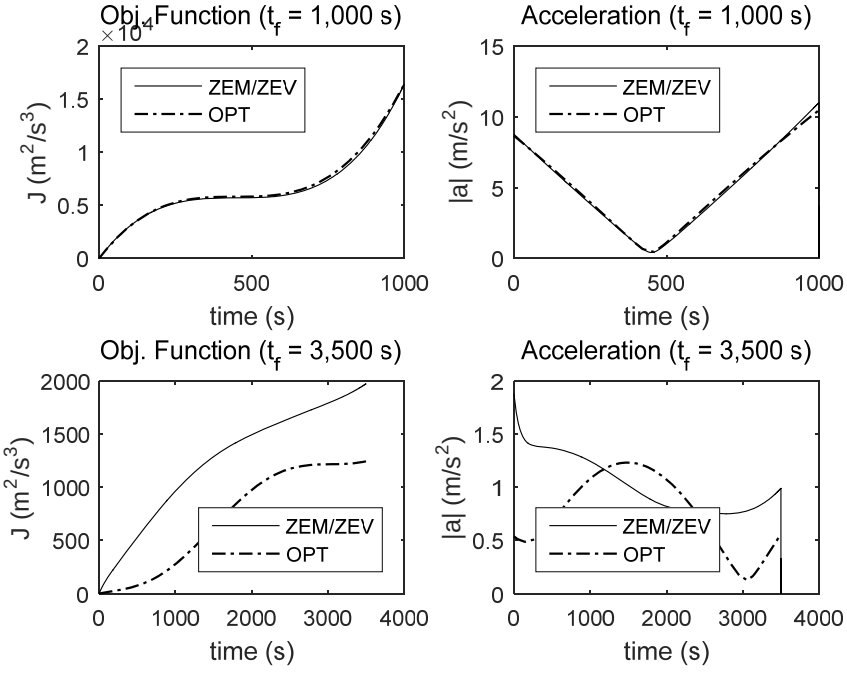

Figure 10: Objective Function and Control Input (t_f = 1,000 / 3,500 sec.)

SUMMARY AND FUTURE WORK

The results of the case studies indicate that the analytic-propagator-based ZEM/ZEV guidance implementation with proposed t_f prediction produces the control input and state profiles very similar to the solutions obtained through an open-loop off-line optimization for relatively long-range missions (flight angle of 90 deg.). The algorithm provides solutions for very-long-range rendezvous problem like Case D (flight angle larger than 180 deg.), but its objective function and input/state profiles were different from those of open-loop optimal solutions. Furthermore, under the assumption of continuous tracking (as was made for case studies), the implementations with different analytic propagators (Kepler and Vinti) do not show meaningful performance difference. Authors expect, however, that in realistic situations in which target's information is not always available during the intercept/rendezvous mission, the advantage of implementation based on Vinti's propagator will be apparent.

Comparison of the proposed algorithm with other feedback guidance laws (e.g. PN guidance and its variants) from the perspectives of the performance and the computational cost can be considered for future work. Use of the proposed algorithm for different applications (e.g. precision landing on a target rotating with the planet) and use of the waypoint-optimized ZEM/ZEV guidance concept [9] as applied to Case D can be another interesting research subject for further exploration.

CONCLUSIONS

This paper has presented a new implementation of the ZEM/ZEV feedback guidance by utilizing the computational efficiency and accuracy of analytic orbital propagators. The problem was formulated as an optimal control problem that minimizes the integral of the control energy with terminal states specified on a plane or a curve, which yields the solution of the ZEM/ZEV feedback control form. A formula to determine the terminal time for the ZEM/ZEV feedback guidance for t_f free problems using the analytic propagator has been developed. The effectiveness of the proposed implementation and optimal terminal-time estimation methodology was demonstrated using missile/spacecraft intercept and rendezvous case studies.

ACKNOWLEDGEMENT

The authors would like to express sincere thanks to Dr. Gim Der who has provided the FORTRAN version of Vinti's propagator, which was directly translated into MATLAB and used for this paper. The authors would also like to thank Ms. Yao Zhang (Ph.D. graduate student at Harbin Institute of Technology) for conducting offline trajectory optimizations for long-range missions of Case D. This work was prepared under a research grant from the National Research Foundation of Korea (NRF-2013M1A3A3A02042461). The authors thank the National Research Foundation of Korea for the support of this research work.

REFERENCES

[1] Bryson, A., and Y. Ho, *Applied Optimal Control*, Wiley, New York, NY, 1969, pp. 154-155.

[2] Battin, R., *An Introduction to the Mathematics and Methods of Astrodynamics*, Revised Edition, AIAA, Reston, VA, 1999, pp. 558-566.

[3] D'Souza, C., "An Optimal Guidance Law for Planetary Landing," AIAA Paper 1997-3709, 1997.

[4] Cho, H., Ryoo, C., and Tahk, M., "Closed-Form Optimal Guidance Law for Missiles of Time-Varying Velocity," *Journal of Guidance, Control, and Dynamics*, Vol. 19, No. 5, 1995, pp. 1017-1022.

[5] Ryoo, C., Cho, H., and Tahk, M., "Optimal Guidance Laws with Terminal Impact Angle Constraint," *Journal of Guidance, Control, and Dynamics*, Vol. 28, No. 4, 2005, pp. 724-732.

[6] Lee, J., Jeon, I., and Tahk, M., "Guidance Law to Control Impact Time and Angle," *IEEE Transactions on Aerospace and Electronic Systems*, Vol. 43, No. 1, 2007, pp. 301-310.

[7] Zarchan, P., *Tactical and Strategic Missile Guidance, Sixth Edition*, AIAA, Reston, VA, 2012, pp. 107-256.

[8] Guo, Y., Hawkins, M., and Wie, B., "Applications of Generalized Zero-Effort-Miss/Zero-Effort-Velocity (ZEM/ZEV) Feedback Guidance Algorithm," *Journal of Guidance, Control, and Dynamics*, Vol. 36, No. 3, 2013, pp. 810-820.

[9] Guo, Y., Hawkins, M., and Wie, B., "Waypoint-Optimized Zero-Effort-Miss/Zero-Effort-Velocity (ZEM/ZEV) Feedback Guidance for Mars Landing, " *Journal of Guidance, Control, and Dynamics*, Vol. 36, No. 3, 2013, pp. 799-809.

[10] Ebrahimi, B., Bahrami, M., and Roshanian, J., Optimal Sliding-Mode Guidance with Terminal Velocity Constraint for Fixed-Interval Propulsive Maneuvers, *Acta Astronautica*, Vol. 62, 2008, pp. 556-562.

[11] Newman, B., "Strategic Intercept Midcourse Guidance Using Modified Zero Effort Miss Steering," *Journal of Guidance, Control, and Dynamics*, Vol. 19, No. 1, 1996, pp. 107-112.

[12] Furfaro, R., Selnick, S., Cupples, M. L., and Cribb, M. W., "Non-Linear Sliding Guidance Algorithms for Precision Lunar Landing," *21st AAS/AIAA Space Flight Mechanics Meeting*, AAS Paper 11-167, 2011.

[13] Vinti, J., Der, G., and Bonavito, A., *Orbital and Celestial Mechanics*, Volume 177, Progress in Astronautics and Aeronautics, AIAA, Reston, VA, 1998, pp. 75-106.

[14] Bate, R., Mueller, D., and White, J., Fundamentals of Astrodynamics, Dover Publications, New York, NY, 1971, pp. 177-222.

[15] Vallado, D., Fundamentals of Astrodynamics and Applications, Microcosm Press, Hawthorne, CA, 2007, pp. 87-103.

[16] Kirk, D., *Optimal Control Theory: An Introduction*, Prentice Hall, Englewood Cliffs, NJ, 1970, pp. 184-209.

[17] Patterson, M., and Rao, A., "GPOPS-II: A MATLAB Software for Solving Multiple-Phase Optimal Control Problems Using hp-Adaptive Gaussian Quadrature Collocation Methods and Sparse Nonlinear Programming," *ACM Transactions on Mathematical Software*, Vol. 41, No. 1, 2014.

[18] *Der Astrodynamics* company website: http://derastrodynamics.com, last access: Jan. 24, 2016.